

Size and mechanical properties of craze zones at propagating crack tips in poly(methyl methacrylate) during fatigue loading

W. Döll, L. Könczöl and M. G. Schinker

Fraunhofer-Institut für Werkstoffmechanik, Wöhlestr. 11, D-7800 Freiburg, FRG

(Received 6 July 1982; revised 2 February 1983)

In specimens of high molecular weight poly(methyl methacrylate) the microregion at the crack tip has been investigated during fatigue crack propagation by applying the optical interference method in a specially constructed experimental set-up. Thus, in the frequency range of 0.4 to 50 Hz the size and contour of the craze zone were directly measured at upper and lower load of the cycles. In contrast to previous assumptions it is established that the maximum craze width at the crack tip and hence the maximum length of stretched fibrils increases strongly with crack propagation rate. The directly measured craze data and also the material parameters indirectly derived by the aid of the Dugdale model are related to those data which have been measured during continuous crack propagation under quasi-static tensile load. The spacings of the fatigue striations on the fracture surfaces are compared with the lengths of the craze zones.

Keywords Craze zone; Dugdale model; fatigue crack propagation; fatigue striations; interference optics; poly(methyl methacrylate)

INTRODUCTION

The macroscopic fatigue crack growth behaviour of various polymers has been intensively studied as can be seen from recent review articles¹⁻³. Using the fracture mechanics approach⁴ the crack growth rate is determined as a function of relative stress intensity factor ΔK_1 (see *Figure 1*). The influences of different parameters, e.g. mean stress, ratio between maximum and minimum stress, frequency and temperature, have been investigated and are usually incorporated into the well known Paris law using empirical parameters. A more substantiated description of the fatigue crack propagation is expected by a closer insight into the processes in the microregion at the crack tip. Since at fracture most of the strain energy release is consumed by plastic deformations, the dimensions of the plastic zone represent some basic parameters. For some thermoplastics the craze process is known to be the relevant plastic deformation process at the crack tip. It is now well established by the aid of direct measurements that under monotonic tensile loading the craze zone size at the crack tip can be described by the Dugdale model⁵ if the appropriate time- and temperature-dependent material properties are taken into account^{6,7}. In fatigue fracture of viscoelastic/plastic materials time- and frequency-dependent⁸ effects may play an important role. Hence, for an adequate theoretical description of the fatigue crack growth behaviour which has been developed⁹ on the basis of the Dugdale model it is essential to have the correct knowledge of the basic parameters involved, e.g. craze zone size, crack opening displacement and Young's modulus. Whilst the indirect determination of these parameters from macroscopic data suffers from restrictions due to the assumptions involved, the directly determined data for fracture under static load are not

necessarily identical with those for fracture under fatigue load¹⁰. For direct measurements of plastic zone sizes at crack tips in glassy thermoplastics the method of optical interference has proved to be a powerful tool which has already been applied in a subsequent inspection of previously fatigue-loaded cracks¹¹⁻¹³. Recently, an experimental set-up has been reported^{13,14} by which in transparent materials the microscopic small crack tip region can be investigated during fatigue crack propagation.

In this paper investigations of the craze zone size during fatigue crack growth in poly(methyl methacrylate) (PMMA) will be presented. PMMA was chosen because it is a very suitable material for interference optics and its crack propagation behaviour and craze zone sizes at static loading have already been fairly well characterized^{6,7,15}, thus giving a basis for comparisons.

EXPERIMENTAL

The measurements of fatigue crack propagation were performed on a commercial-grade PMMA (Plexiglas 233) with a weight average molecular weight of about 2×10^6 . Compact tension specimens, with characteristic dimensions $8 \times 8 \times 4 \text{ mm}^3$, were machined from cast sheet material and were slotted to a depth of 1.5 mm beyond the loading points with a 0.5 mm thick slitting saw. One side of the specimens, parallel to the crack plane, was polished to enable optical observations. Cracks were started by slowly pushing a razor blade into the notch and sharpened by fatigue loading at 200 Hz. The specimens thus prepared were tested under sine-wave cyclic tensile load at the following frequencies: 0.4, 2, 10 and 50 Hz. The lower load limit was slightly in the tensile region (about 5% of the upper tensile load), in order to avoid moving the

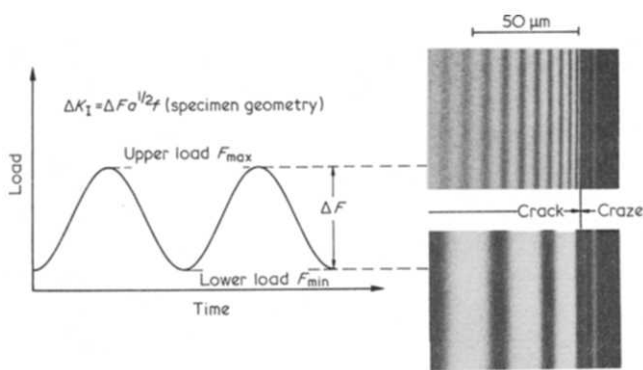


Figure 1 Effect of fatigue loading on interference fringe pattern in PMMA at upper and lower load: $\Delta K_I = 12.0 \text{ N mm}^{-3/2}$ ($= 0.38 \text{ MN m}^{-3/2}$), $da/dN = 1.2 \times 10^{-5} \text{ mm/cycle}$, $\omega = 50 \text{ Hz}$

specimen. The applied ΔK_I values were in the range of 10 to $35 \text{ N mm}^{-3/2}$ (0.32 to $1.1 \text{ MN m}^{-3/2}$) and the resulting crack speeds \dot{a} varied from 10^{-6} to $10^{-2} \text{ mm s}^{-1}$ depending on test frequency. All tests were performed at a temperature of 23°C and a relative humidity of 50%.

The optical interference investigations of the craze at the crack tip in the fatigue-loaded PMMA specimen were performed with a specially constructed experimental set-up. Since it has been described in detail previously^{13,14}, here only the main features are summarized.

Naturally, the optical method used is in principle the same as that already applied to static^{6,16} and to continuously moving¹⁵ cracks under static load. However, during crack propagation under oscillating fatigue load the transient and spatial rapidly changing microscopic image of the interference fringe pattern has to be recorded. This is achieved by a monochromatic stroboscopic and flash illumination respectively in combination with adequate triggering. By the aid of a phaseshifting system it is possible to record the interference fringe pattern at any desired phase of the load cycle.

It must be emphasized that by this experimental arrangement the following relevant parameters can be recorded simultaneously:

- (1) interference pattern,
- (2) acting load,
- (3) number of load cycles,
- (4) frequency or period of the wave,

and hence the following correlated parameters can be deduced:

- (a) craze zone size (craze length and width),
- (b) stress intensity factor K_I ,
- (c) crack propagation rate da/dN ,
- (d) crack speed \dot{a} .

Thus a full characterization of the crack and craze growth under cyclic loading is possible.

Figure 1 shows examples of photographed interference fringe systems generated at a fatigue frequency of 50 Hz and a crack speed \dot{a} of $5.9 \times 10^{-4} \text{ mm s}^{-1}$. The direction of crack propagation is from left to right and the still unbroken material appears dark since the interferences are observed in reflected light. The two different fringe systems due to craze width and crack opening can clearly be discerned. The influence of lower and upper load on the craze width and crack opening can be roughly estimated

by the number and the local density of fringes, respectively.

For the exact calculation of the craze contour from the interference fringes such photographs of fringe systems were first scanned in a microdensitometer to determine the positions of the individual fringes accurately. For the calculation of the craze thickness a knowledge of the refractive index of the craze and its variation with strain is required, and can be estimated, following Brown and Ward⁶, with the aid of the Lorentz-Lorenz equation, together with the measured numbers of fringes in the unloaded and loaded craze and using the value of the refractive index of the unloaded craze¹⁷.

THE DUGDALE MODEL

Owing to the high stresses around the tips of loaded cracks the material in that region undergoes plastic deformation. A model to describe the shape and size of this yielded region at the crack tip was developed by Dugdale⁵. The model considers a loaded crack which is terminated by a plastic zone whose length s is defined by the condition that there should be no stress singularity at the tip of the plastic zone. Under this condition, and with the additional restriction that the applied stress σ is small compared to the constant assumed yield stress σ_y of the material, s is given, to a very good approximation, by

$$s = \frac{\pi K_I^2}{8 \sigma_y^2} \quad (1)$$

where K_I is the stress intensity factor for the crack opening mode.

An analytical expression was derived by Goodier and Field¹⁸ for the displacements $2v(x)$ of the elastic-plastic boundary ($x = \text{coordinate parameter}$). Since this expression has a complicated form, a simpler expression is usually considered for the displacements of the plastic zone boundaries, which has been derived by Rice¹⁹. For small plastic zones and under plane strain it has the form:

$$2v(x) = \frac{8 \sigma_y (1 - \nu^2)}{\pi E} \left[\xi - \frac{x}{2s} \ln \left(\frac{1 + \xi}{1 - \xi} \right) \right] \quad (2)$$

where $\xi = (1 - x/s)^{1/2}$, $E = \text{Young's modulus}$ and $\nu = \text{Poisson's ratio}$.

The displacement at the crack tip $2v(0) = 2v$ is given by

$$2v = \frac{K_I^2 (1 - \nu^2)}{\sigma_y E} \quad (3)$$

As mentioned above it has been shown by different authors^{6,7,16} that the Dugdale model is suitable for describing the craze zone at the crack tip in a glassy thermoplastic.

Figure 2 shows an example of the application of the Dugdale model to the craze zone at the crack tip. The experimental points of craze zone and crack opening are given as open circles. Whilst the position of the crack tip is known exactly, the location of the craze tip and hence the craze length s cannot be measured directly, but can only be obtained by extrapolation. The extrapolation method applied here used all the experimental points for a particular craze together with equations (1) and (2) to calculate by iteration that value of s (and hence the corresponding values of E and σ_y) which minimized the variation in E along the length of the craze.

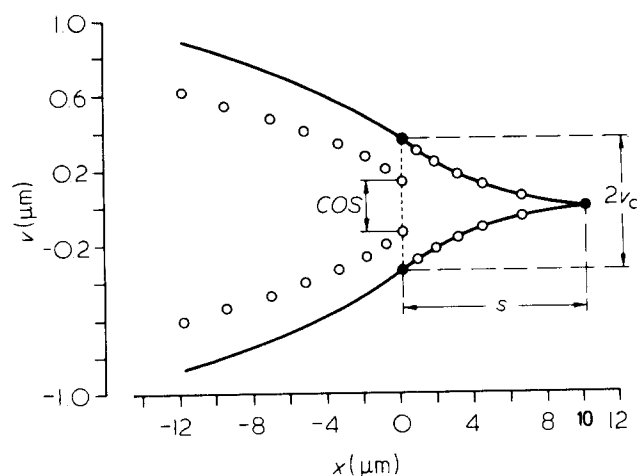


Figure 2 Example of measured craze shape and crack opening in PMMA under fatigue loading: $\Delta K_I = 12.0 \text{ N mm}^{-3/2}$ ($= 0.38 \text{ MN m}^{-3/2}$), $\omega = 50 \text{ Hz}$, $da/dN = 1.2 \times 10^{-5} \text{ mm/cycle}$. The drawn line represents the fit by the Dugdale model

The position of the craze tip thus extrapolated is shown in *Figure 2* as a closed circle. Also shown are the lines corresponding to the displacements $2v(x)$ as calculated by the formulae of Rice¹⁹ and Goodier and Field¹⁸ using the fitted values of s , E and σ_y . Comparing the calculated with the measured values it can be seen that there is good agreement in the craze zone (as might have been expected) but the calculated curve for the crack opening is displaced from the experimental points. This apparent discrepancy between the Dugdale model and the experimentally determined crack opening is removed, however, if it is taken into account that the model provides the locus of the displacements of the elastic-plastic boundary not only ahead of the crack tip but also behind it. This means, in the case of PMMA, that to the measured crack opening must be added the thickness of the layer of crazed material which remains on the fracture surfaces. Hence, in the case of a thermoplastic material it is especially important to distinguish at the location of the crack tip between true crack opening stretch ($= \text{COS}$) and maximum craze width $2v$. To characterize the plastic deformation and fracture behaviour of a thermoplastic material the maximum length of stretched fibrils and hence maximum craze width $2v$ is the more fundamental parameter. At fracture, when a critical maximum craze width is reached, it will be indicated by $2v_c$.

RESULTS AND DISCUSSION

The crack propagation behaviour under fatigue loading is usually measured as the increase in crack length, da , per number of cycles, dN , versus relative stress intensity factor ΔK_I ($= \Delta F a^{1/2} f$, where a = crack length and f = dimensionless coefficient; see *Figure 1*). In *Figure 3a* the results for high molecular weight PMMA are combined for all four frequencies; every point shown is based on nearly 40 measurements. The course of the curve is in general agreement with the results of other investigators^{20,21,9}.

For different polymers the influence of frequency has been extensively reported¹, by which the fatigue crack propagation rate decreases with increasing frequency. A

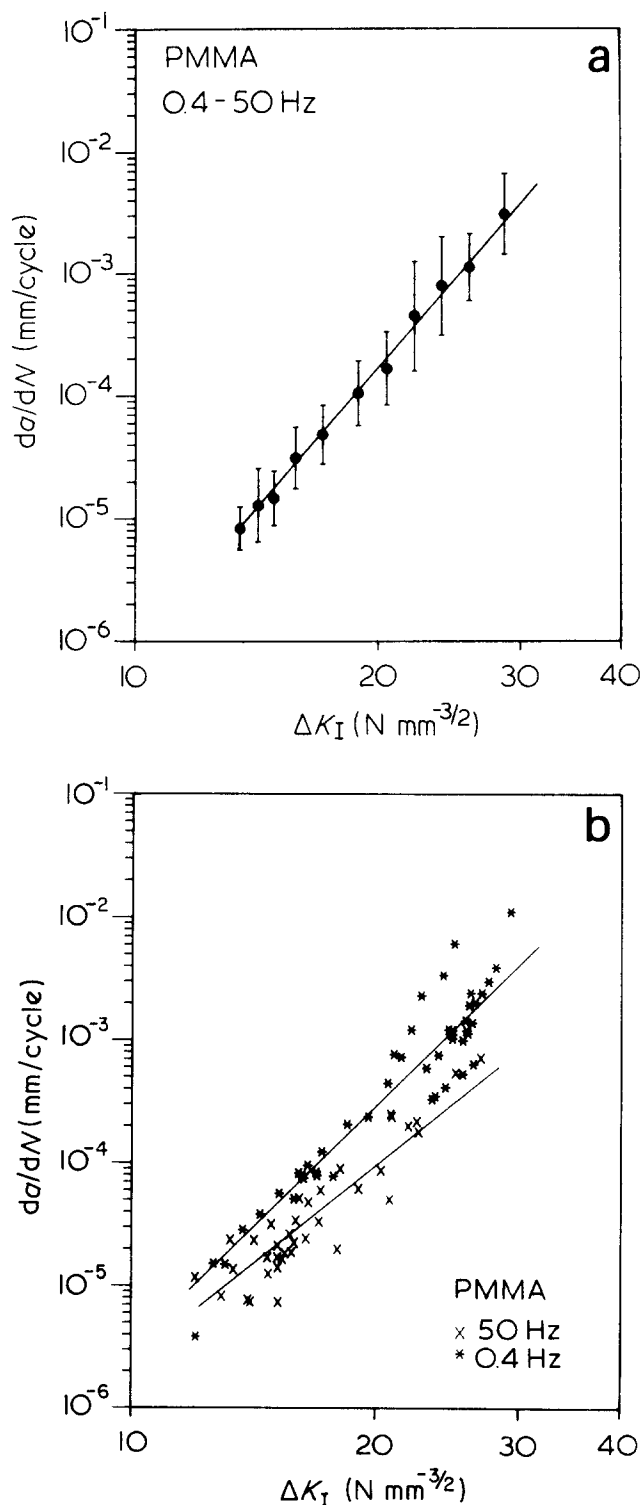


Figure 3 Crack propagation rate da/dN versus relative stress intensity factor ΔK_I ($1 \text{ MN m}^{-3/2} = 31.62 \text{ N mm}^{-3/2}$): (a) Curve summarized for all four frequencies; every point is an average of about 40 measurements. (b) Course of two curves with their individual data points

frequency sensitivity factor (*FSF*) has been defined^{22,1} as the multiple by which the fatigue crack propagation rate changes per decade change in test frequency. For high molecular weight PMMA an *FSF* is reported¹ to be between 2.5 and 3.3.

The PMMA material investigated here shows only a small influence of frequency. This can be concluded already from the scatter band of the curve in *Figure 3a* and

is shown explicitly in Figure 3b for the curves of 0.4 and 50 Hz which exhibit the largest differences in crack propagation behaviour. Even in this case only a small *FSF* of at most 1.2 can be derived. At the moment, the reason is not clear for the discrepancy between the results here and those mentioned above.

Whilst Figure 3 shows the macroscopic fatigue crack growth behaviour, Figure 4 sheds light on the material behaviour in the microregion at the crack tip by presenting the maximum craze width $2v_c$ as function of crack propagation rate, da/dN . It can be stated clearly that during fatigue crack propagation the maximum craze width $2v_c$ (and hence also *COS*) is not constant, as usually assumed up to now but increases by a factor of nearly 5 from $0.6 \mu\text{m}$ to about $2.8 \mu\text{m}$ in the predominantly investigated crack propagation range of 10^{-5} to 10^{-2} mm/cycle. Figure 4 indicates a lower limit of $2v_c$ at crack propagation rates smaller than 10^{-5} mm/cycle; a statement on an upper limit cannot be derived from the course of the curve. It is of interest to compare the maximum craze width $2v_c$ measured during fatigue crack propagation with those determined during continuous crack propagation under constant load. For the two different types of loading the crack speed \dot{a} is used as a common measure. Since \dot{a} is equal to $\omega da/dN$ (ω =frequency) the original curve of $2v_c$ in Figure 4 is separated in Figure 5 according to the different frequencies in the way that at lower frequencies the increase in $2v_c$ occurs at lower crack speeds \dot{a} . At the top of Figure 5 the maximum craze width $2v_c$ measured for continuously moving cracks is shown which has a nearly constant value of $2.7 \pm 0.2 \mu\text{m}^{15}$. This 'quasi-static curve' obviously forms the upper limit of maximum craze width $2v_c$ which can be attained under fatigue loading. At the various frequencies this limiting curve is reached at different crack speeds. These speeds differ by nearly the same factor as do the frequencies, that is the upper limit of craze size is reached at the same crack propagation rate of about 10^{-2} mm/cycle for all frequencies. The craze length s is given in Figure 6 as a function of crack propagation rate da/dN . Length s increases from

about $10 \mu\text{m}$ up to about that value measured at continuously propagating cracks, namely $s = 35 \pm 3 \mu\text{m}^{15}$. It should be mentioned that the craze lengths reported previously¹³ are larger than those given here due to the extrapolation of s at a craze in the unloaded state which leads to an overestimation.

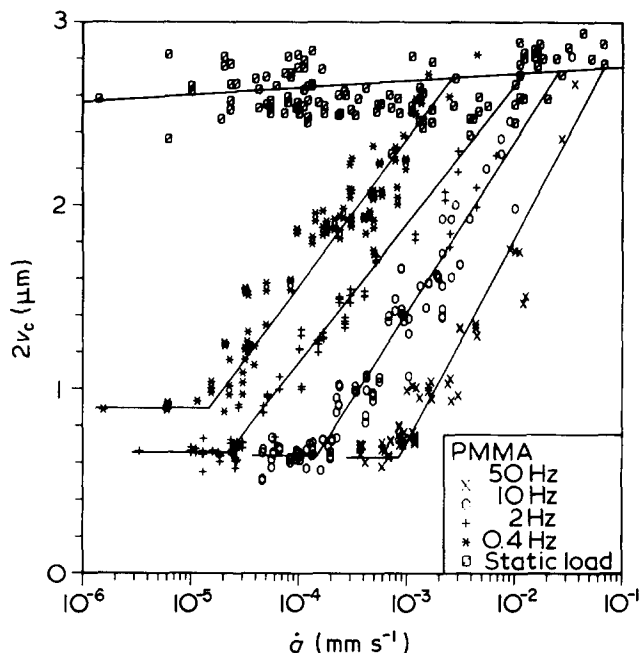


Figure 5 Maximum craze width $2v_c$ as function of crack speed \dot{a} ; reference curve (at the top) is due to continuously moving cracks under quasi-static load

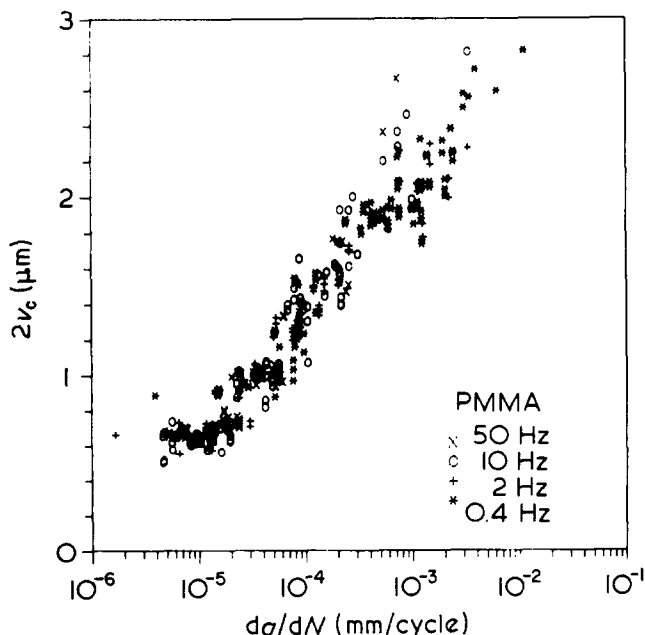


Figure 4 Maximum craze width $2v_c$ at the crack tip (compare Figure 2) as function of crack propagation rate da/dN

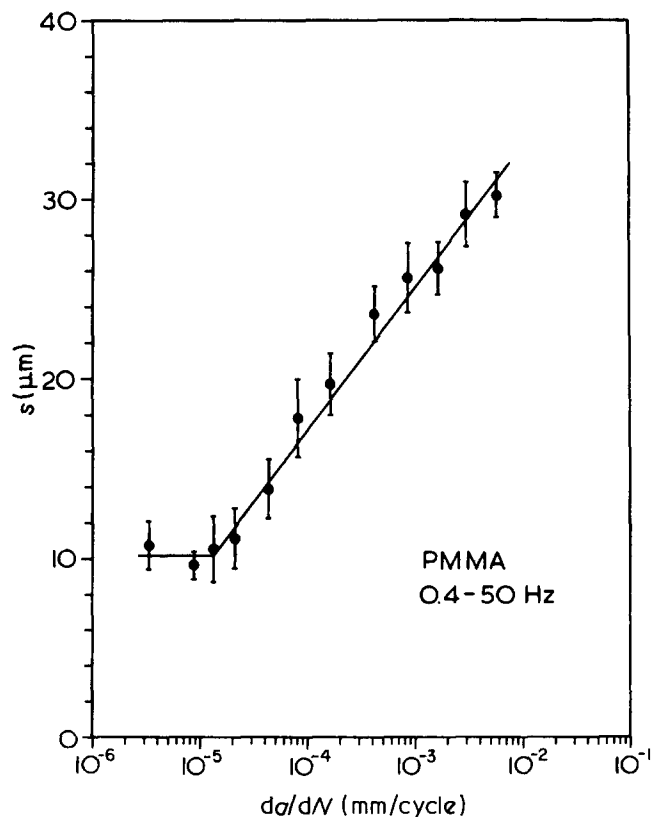


Figure 6 Craze length s (compare Figure 2) as function of crack propagation rate da/dN

Having analysed craze width and length separately it is interesting to investigate the growth behaviour of both parameters. In Figure 7 maximum craze width $2v_c$ is plotted against craze length s ; additionally to the individual data points of fatigue crack propagation the data of continuously moving cracks are included as the large circle, consisting of 113 measurements. It can be seen from Figure 7 that the craze dimensions—maximum width and length—increase almost proportionally to each other up to that value determined for continuous crack propagation under constant load. It is apparent that the increase in craze length takes place by the fibrillation process of the amorphous bulk polymer. However, the thickening of the craze may be due to an additional fibrillation or to an enhanced stretching of already formed fibrils or even to both processes. In this context it should be mentioned that investigations on craze growth in thin polymer films of polystyrene²³ and polycarbonate²⁴ under quasi-static tensile load led to the result that the increase in craze width occurs by fibrillation of fresh bulk material. It should be emphasized that there are differences between both types of experiments: whilst in the fatigue crack growth experiments crazes of different sizes are compared which were generated by different load histories (ΔK_I , da/dN , ω), in the experiments referred to the increases in craze size were performed on the same single craze.

In order to get further information on the craze thickening behaviour the widths $2v_0$ at the crack tips of the unloaded crazes were measured which give direct information of the amount of fibrillation. In Figure 8, $2v_0$ is plotted together with the maximum craze width $2v_c$ as functions of da/dN . It can be deduced from Figure 8 that both processes—new craze material being formed and also a larger stretching of the fibrils—occur with an increasing crack propagation rate. If the strain in the craze zone is defined by $\epsilon = (2v_c - 2v_0)/(2v_0)$ then the strain on the fibrils is nearly doubled from about 70% at low crack propagation rates of 10^{-5} mm/cycle up to 120% at 10^{-2} mm/cycle, tending to a magnitude measured for continuously propagating cracks²⁵.

It is well known that fatigue crack propagation may be associated with markings on the fracture surface. In

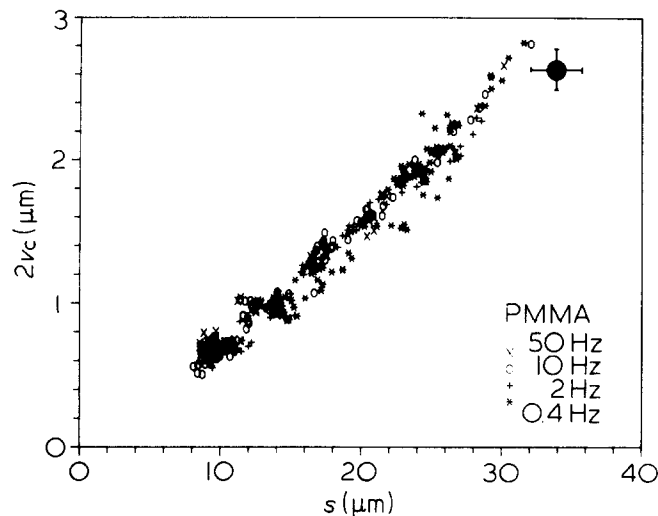


Figure 7 Relationship between maximum craze width $2v_c$ and craze length s at crack propagation under fatigue and quasi-static (circular area) loading

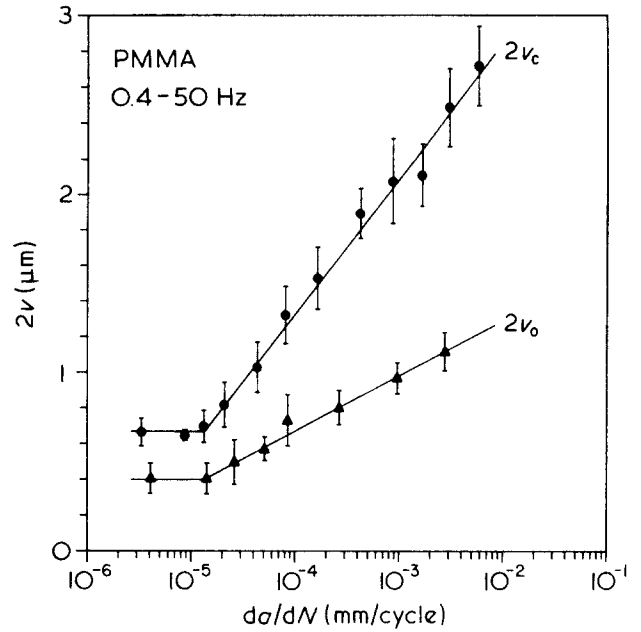


Figure 8 Craze width at the crack tip ($2v_c$ under upper and $2v_0$ under lower load) as function of crack propagation rate da/dN

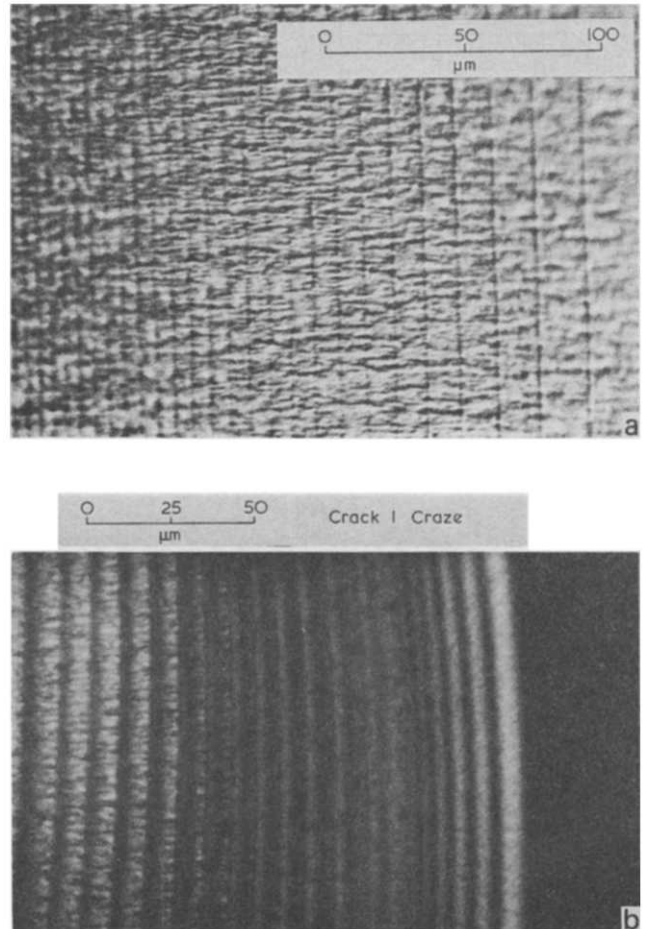


Figure 9 Fatigue lines on PMMA fracture surfaces. Crack propagation direction from left to right. (a) Light optical photograph of a broken specimen. (b) Optical interference photograph of fracture surface and craze zone in a partially broken specimen

Figure 9a an example is shown of fatigue arrest lines with increasing distances due to an accelerating crack. It is known from the literature¹ and it was also observed here that in high molecular weight PMMA one loading cycle causes one increment in crack advance. The distances of the fatigue striations have often been correlated to the plastic zone size, especially its length. A direct comparison between striation spacing and length of the craze zone can be made from the optical interference picture shown in Figure 9b. The crack was first driven by $\Delta K_I = 32 \text{ N mm}^{-3/2}$ ($\approx 1 \text{ MN m}^{-3/2}$) at a loading frequency of 10 Hz and moved by a speed \dot{a} of nearly $10^{-1} \text{ mm s}^{-1}$; it was then arrested by unloading. (This was necessary to get a sharp picture of both, striations on the fracture surface and interference fringes.) It can be seen that in this case the craze length is significantly larger than the striation spacing. A direct comparison between craze dimensions and line spacing can be deduced from Figure 10. Here craze length s (upper curve) and maximum craze width $2v_c$ (lower curve) are plotted against crack propagation rate da/dN in a comparable scale since in high molecular weight PMMA the crack growth during one cycle corresponds to one increase in line spacing. The broken lines indicate in which regions the dimensions of the craze would directly correspond to the line spacing. Thus the slope at 45° indicates where the increase in crack length during one cycle is equal to the craze dimensions. It can be seen from Figure 10 that up to about $2 \times 10^{-3} \text{ mm}$ even the craze width is larger than the increase in crack length during one cycle. Only at high crack propagation rates ($> 3 \times 10^{-2} \text{ mm/cycle}$) will the increments in crack length be larger than the craze length. It will also be expected that at higher crack propagation rates there will always be a craze zone in front of the crack tip, as has already been observed at high speeds of continuously moving cracks^{1,5}. At low crack propagation rates it is interesting to note that the dimensions of the craze zone are also constant. An increase of craze dimensions seems to begin at nearly $2 \times 10^{-5} \text{ mm/cycle}$. Since the fibril diameter of high molecular weight PMMA has been determined²⁶ to be

about $2.5 \times 10^{-5} \text{ mm}$ the lower bound of craze dimensions may be associated with a crack propagation rate of one fibril diameter per fatigue cycle. This hypothesis has to be checked with other materials.

It is well established that the stress on the craze zone σ_y and the Young's modulus E can be derived from the measured craze dimensions by the aid of the Dugdale model in applying equations (1)–(3) using the procedure described above. In Figure 11 the derived yield stresses σ_y are plotted as function of crack speed \dot{a} in order to allow these data of fatigue crack growth to be compared with those of continuously moving cracks⁷ given by the straight line. In the investigated crack speed range σ_y increases from about 70 to 110 MPa and the general tendency of the data determined under fatigue and static loading seems to be quite similar. However, a closer analysis reveals slight differences for the different frequencies concerning two points: first, the data of the particular frequencies are assembled in different crack speed ranges, and secondly, the slopes of the individual curves become flatter with increasing frequency and are almost constant for 10 and 50 Hz.

The magnitude of the Young's modulus is in the same range as that measured during continuous crack propagation; however, the data of fatigue crack propagation do not show a significant change with crack speed. As can be seen from Figure 12 a slight increase of the modulus E with frequency may be stated which has been reported²⁷ for moduli measured under small strains. Since the values of the latter lie about 50% higher than the values determined here, one has to conclude that the moduli here must be characteristic for large strains. This conclusion becomes even more evident if it is recognized that the material around the craze zone is highly strained due to the high stresses around the crack tip and that the Dugdale model describes the contour of the elastic/plastic boundary in that region.

In this context it is interesting to mention a dispute between different authors^{9,27,28} concerning the applicability of a fatigue crack growth model in polymers. In his

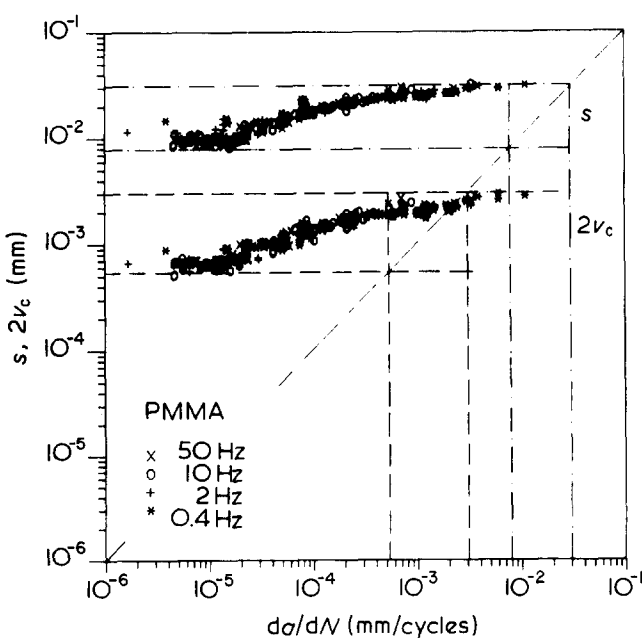


Figure 10 Characteristic craze dimensions s and $2v_c$ versus crack propagation rate da/dN

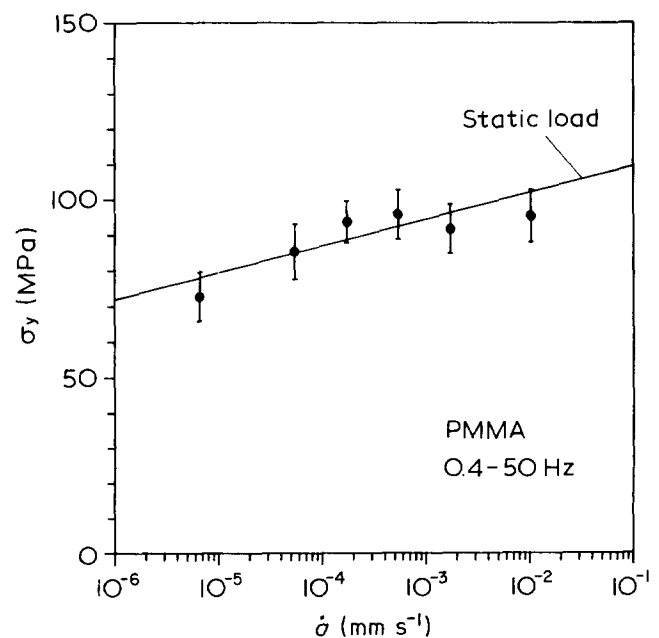


Figure 11 Yield stress σ_y at fatigue and static loading as function of crack speed \dot{a}

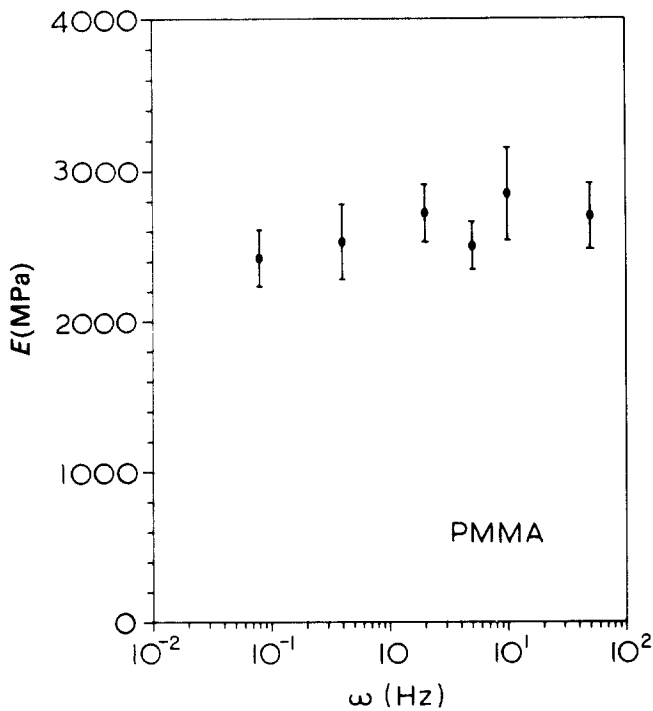


Figure 12 Modulus E versus loading frequency ω

model, Williams⁹ used a two-stage craze zone in which the newly formed craze material in a small region at the craze tip experiences a very high stress while the main part of the craze sustains a much lower stress. Referring to experimental values for crazing stresses of a number of polymers Hertzberg *et al.*²⁷ suggest that in these cases the craze experiences a uniform stress similar to that postulated in the Dugdale model. The experimental data on high molecular weight PMMA of this work, especially the analysis of the measured craze contours, show that an excellent fit will be reached by a uniform stress in the Dugdale model. Furthermore, our results also clearly show that the basic assumption of the two-stage model—a constant crack opening displacement—must be modified.

Summing up, it can be stated that the optical interference investigations of fatigue crack propagation in high molecular weight PMMA have led to the following results.

The craze dimensions are not constant in the investigated crack propagation range:

- (a) craze width $2v_c$ and craze length s increase by a factor of about 5 with increasing crack propagation rate, showing maximum and minimum values at the upper and lower end of the crack propagation range;
- (b) the upper values tend to those determined at continuously moving cracks under constant load;
- (c) the lower limit corresponds to an increment in crack growth of one fibril diameter per fatigue cycle;

- (d) the increase in craze dimensions with crack propagation rate seems to occur by an additional fibrillation of bulk material and by a larger stretching of the fibrils.

The yield stress increases with crack speed in a similar way as for continuously moving cracks under constant load.

The modulus is practically constant with crack speed, its magnitude corresponding to a modulus measured under high strains.

There is no simple correlation between fatigue striation spacing and craze length.

An influence of loading frequency on crack propagation rate and craze dimensions is hardly discernible.

ACKNOWLEDGEMENT

The financial support by the DFG (Deutsche Forschungsgemeinschaft) is gratefully appreciated.

REFERENCES

- 1 Hertzberg, R. W. and Manson, J. A. 'Fatigue of Engineering Plastics', Academic Press, New York, 1980
- 2 Sauer, J. A. and Richardson, G. C. *Int. J. Fracture* 1980, **16**, 499
- 3 Radon, J. C. *Int. J. Fracture* 1980, **16**, 533
- 4 Paris, P. C. and Erdogan, F. *J. Bas. Eng., Trans. ASME (Ser. D)* 1963, **85**, 528
- 5 Dugdale, D. S. *J. Mech. Phys. Solids* 1960, **8**, 100
- 6 Brown, H. R. and Ward, I. M. *Polymer* 1973, **14**, 469
- 7 Döll, W., Seidelmann, U. and Könczöl, L. *J. Mater. Sci.* 1980, **15**, 2389
- 8 Feltner, C. E. *J. Appl. Phys.* 1967, **38**, 3576
- 9 Williams, J. G. *J. Mater. Sci.* 1977, **12**, 2525
- 10 May, Y. W. and Williams, J. G. *J. Mater. Sci.* 1979, **14**, 1933
- 11 Mills, N. J. and Walker, N. *Polymer* 1976, **17**, 335
- 12 Pitman, G. and Ward, I. M. *J. Mater. Sci.* 1980, **15**, 635
- 13 Schirrer, R., Schinker, M. G., Könczöl, L. and Döll, W. *Colloid Polym. Sci.* 1981, **259**, 812
- 14 Döll, W., Schinker, M. G. and Könczöl, L. 'Deformation, Yield and Fracture of Polymers', Plastics and Rubber Institute, 1982, p.20.1
- 15 Schinker, M. G. and Döll, W. in 'Mechanical Properties at High Rates of Strain', Conf. Ser. No.47, Institute of Physics, Bristol, 1979, p.224
- 16 Weidmann, G. W. and Döll, W. *Colloid Polym. Sci.* 1976, **205**, 254
- 17 Kambour, R. P. *Polymer* 1964, **5**, 143
- 18 Goodier, J. N. and Field, F. A. in 'Fracture of Solids', (eds D. C. Drucker and J. J. Gilman), Interscience, New York, 1963, p.103
- 19 Rice, J. R. in 'Fracture', (ed. H. Liebowitz), Academic Press, New York, 1968, vol.II, p.191
- 20 Watts, N. H. and Burns, D. J. *Polym. Eng. Sci.* 1967, **7**, 90
- 21 Hertzberg, R. W., Nordberg, H. and Manson, J. A. *J. Mater. Sci.* 1970, **5**, 521
- 22 Hertzberg, R. W., Manson, J. A. and Skibo, M. *Polym. Eng. Sci.* 1975, **15**, 252
- 23 Lauterwasser, B. D. and Kramer, E. J. *Philos. Mag. A* 1979, **39**, 469
- 24 Verheulpen-Heymans, N. *Polymer* 1979, **20**, 356
- 25 Döll, W. and Weidmann, G. W. *Progr. Colloid Polymer Sci.* 1979, **66**, 291
- 26 Paredes, E. and Fischer, E. W. *Makromol. Chem.* 1979, **180**, 2707
- 27 Hertzberg, R. W., Skibo, M. D. and Manson, J. A. *J. Mater. Sci.* 1979, **14**, 1754
- 28 Williams, J. G. *J. Mater. Sci.* 1979, **14**, 1758